Mine Water and the Environment (2004) 23: 20–27 © IMWA Springer-Verlag 2004

Technical Article

Buffering of Acidic Mine Lakes: The Relevance of Surface Exchange and Solid-Bound Sulphate

W. Uhlmann[1], H. Büttcher[1], O. Totsche[2], and C.E.W. Steinberg[2]

[1]Institute for Water and Soil, Langobardenstraße 48, D-01239 Dresden, Germany [2]Leibniz-Institute of Freshwater Ecology and Inland Fisheries, Müggelseedamm 301, D-12587 Berlin, Germany; Dr. Uhlmann's e-mail: iwb.dresden@t-online.de

Abstract. Buffering mechanisms in an acidic mine lake in Lusatia, Germany were investigated. The titration curve has four sections with different buffering mechanisms: (1) buffering by free hydrogen ions and hydrogen sulphate (pH = 2.55-2.9), (2) buffering by Fe with bound SO_4 (pH = 2.9-4.3), (3) buffering by Al with bound SO_4 (pH = 4.3-5.5), and (4) buffering by surface exchange of SO_4 and basic cations (pH > 5.5). Three different phase models were applied to simulate the titration curve: (1) an iron and aluminium hydroxide model; (2) an iron and aluminium hydroxysulphate model; and (3) an iron hydroxide model with surface exchange for SO_4, Ca, and Mg, coupled with an aluminium hydroxysulphate model. The uncertainty of model input parameters was accounted for in a sensitivity analysis. Only the third model, which considers surface exchange, was able to adequately reproduce the measured titration curve.

Key words: acidic mining lakes; Lusatia; pH buffering; PHREEQC modelling; surface complexation; titration

Introduction

Lakes that develop in lignite open pits after mining due to natural groundwater rebound are often characterised by a low pH and high concentrations of Fe, Al, and SO_4 due to acid input from mine waste and adjacent groundwater bodies (Schnoor et al. 1997; Grünewald 1999). Three possible remediation strategies for these lakes are: flooding with alkalinity-buffered surface waters from regional rivers; chemical treatment with alkaline substances such as limestone, lime, or sodium hydroxide; and the promotion of biological reductive processes (Klapper et al. 1998; Skousen et al. 1998; Uhlmann et al. 2001; Totsche and Steinberg 2003). The objective of all of these strategies is the long-term decrease and elimination of acidity in the mine lakes, thereby increasing the pH to circumneutral values.

In the extremely acidic mining lakes in Lusatia, north-eastern Germany, acidity [titrated to pH 4.3 (hereafter referred to as base neutralization capacity or $BNC_{4.3}$)] values reach up to 10 – 15 mmol L^{-1} and, in extreme cases, up to 30 mmol L^{-1}, due to high concentrations of dissolved ferric iron and aluminium (Nixdorf et al. 2001; Nixdorf et al. 2003). These lakes are characterised by pH values between 2 and 4 and are mainly Fe buffered (Klapper at al. 1996; Geller et al. 1998). A few lakes are aluminum buffered, with pH values in the range of 4 to 5, similar to lakes affected by acid rain (Ulrich 1981).

Buffering characteristics can be described by titration curves. These curves relate pH to acidity and have previously been used in the context of acidic mining lakes (Fyson and Kalin 2000; Totsche et al. 2002). In this study, the titration curve of acidic water from a mine lake in Lusatia was investigated in detail. The objective was to obtain a detailed understanding of buffering mechanisms relevant to lake water neutralisation as well as a quantitative description by hydrochemical modelling. Phases precipitated during titration were analysed by standard analytical methods as well as mineralogical structure analyses (Totsche et al., submitted).

Material and Methods

The study was performed on water samples from the epilimnion of the Plessa 111 mine lake in Lusatia, north-eastern Germany. The lake developed by natural groundwater rebound after mining ended in 1956. The lake is 110,000 m^2 in area, with a maximum depth of about 10 m. It has a pH of 2.55, a $BNC_{4.3}$ of ≈ 10 mmol L^{-1} (and a $BNC_{8.2}$ of 15.5 mmol L^{-1}), and high dissolved iron (ca. 150 mg L^{-1}), aluminium (ca. 30 mg L^{-1}), and sulphate (ca. 1300 mg L^{-1}), which is typical for acid mining lakes in Lusatia (Nixdorf et al. 2001).

The acidic water was titrated with 0.1 N NaOH using an automatic titrator and continuous stirring. Titrations were carried out continuously and discontinuously. During discontinuous titrations, a defined amount of base was added at every step. After adding the base, mixing was stopped and precipitates were collected in sediment traps and removed.

Water samples were filtered with a 0.45 µm sodium acetate filter by compressed air. Water samples were analysed for dissolved Fe, Al, Mn, Ca, and Mg by atomic absorption spectrometry (AAS 3300, Perkin Elmer), for Na and K by atomic emission spectrometry

(AAS 3300, Perkin Elmer), and for SO_4 and Cl by a Shimadzu ion chromatography system. Fe^{2+} was analysed photometrically (Photometer UV 2101, Shimadzu) using the 1,10-phenanthroline method. Precipitates were dried for about 40 hours at 105°C and ground with mortar and pestle before analysis. Solid phase samples were analysed for Fe, Al, Mn, Ca, Mg, Na, K, and total S.

The titration curve was simulated using the geochemical simulator PHREEQC (Parkhurst and Appelo 1999). Three different equilibrium phase models were applied. In the simplest model, the precipitating phases were iron and aluminium hydroxide, and manganese oxide. In the second model, iron and aluminium hydroxysulphate took the place of the hydroxide phases. The third model accounted for surface complexation. For Fe, a hydroxide model with sorptive attributes, which considers the pH-dependent protonation and deprotonation of hydroxyl groups as well as adsorption and desorption of SO_4, Ca, and Mg, was applied. Thermodynamic constants for surface complexation on hydrous ferric oxides were taken from Dzombak and Morel (1990). For Al, the hydroxysulphate model was applied, as in phase model (2), as thermodynamic constants for surface complexation were not available in the PHREEQC data set. For Mn, the oxide model was applied, as in phase models (1) and (2).

The models all assume a constant partial pressure for oxygen, guaranteeing oxic conditions in the model as in the experiment. CO_2 gas exchange was not accounted for in the standard model, but its effects were investigated in a special consideration.

Results and Discussion

Experiments

Titration experiments were performed six times using the same water sample. Titration curves were highly congruent (data not shown). On the whole, about 100 titration curves were recorded, all based on lake 111 water samples. The curves differ only slightly depending on the pH, and the Fe and the Al concentrations. The time span of the continuous titration was ≈ 15 hours. However, we found no significant time dependency in the titration curves using other time intervals between hours and days.

The detectable inorganic carbon (TIC) concentration in the mine water was below 0.5 mg L^{-1}. This is in accordance with TIC measurements in most of the pit lakes in Lusatia, which show TIC concentrations in equilibrium with the atmospheric partial pressure (≈$10^{-3,5}$ bars) of approx. 0.2 – 0.3 mg L^{-1}.

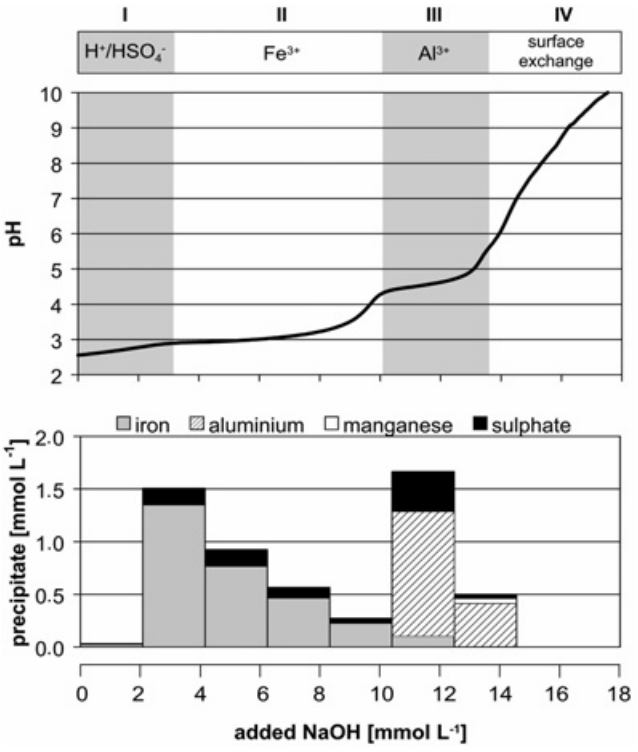

Figure 1. Measured titration curve of the acidic lake water and composition of the precipitates; the grey shades denote the different buffering sections

During the titration experiments, the redox potential was measured continuously. The initial measurements (Eh ≈ + 790 mV) show oxic conditions and the predominance of Fe^{3+}. The detectable Fe^{2+} concentration in the lake water was below 0.05 mg L^{-1}. The measured titration curve of the acidic lake water is shown in Figure 1. Additionally, the main constituents of the precipitates, obtained in seven steps, are depicted.

The titration curve can be divided into four sections. In section I (0.0 – 3.0 mmol L^{-1} NaOH added), the pH increased continuously, from 2.55 to 2.9. Precipitation was negligible. In general, a pH rise from 2.55 to 2.9 is associated with a decrease of the free hydrogen ion concentration of about 1.5 mmol L^{-1}. Thus, about 1.5 mmol L^{-1} of the 3.0 mmol L^{-1} base added in this section was solely consumed by the neutralisation of hydrogen ions. The remaining base added was used for the deprotonation of hydrogen sulphate as well as for the homogeneous hydrolysis of iron.

In section II (3.0 – 10.0 mmol L^{-1} NaOH added), the pH was nearly constant at pH ≈ 3. An orange iron hydroxysulphate, with a mean Fe/S molar ratio of 5.6:1, precipitated. The Fe/S molar ratio is in the range of that typically found for schwertmannite (Bigham et al. 1990). Mineralogical analyses (infrared and x-ray diffraction) confirmed that schwertmannite was present (Totsche et al., submitted). After the plateau, there was a short and weakly buffered transitional

section in which the pH rose to 4.3. Section II was dominated by Fe buffering, as dissolved Fe^{3+} in the acidic water hydrolysed and precipitated. The process releases hydrogen ions, delaying a further rise of pH.

In section III (10.0 – 13.5 mmol L^{-1} NaOH added), a second plateau occurred (pH = 4.3 to 5.5) due to Al buffering. A white sediment with an Al/S molar ratio of 2.7:1 precipitated. Based on the sulphur content, the precipitate was aluminium hydroxysulphate. Since the precipitate was x-ray amorphous, further mineralogical analyses was not possible. The stoichiometry, however, is in the range of known aluminium hydroxysulphate minerals, such as basaluminite, with an Al/S molar ratio of 4:1.

In section IV (> 13.5 mmol L^{-1} NaOH added), the pH increased relatively linearly, starting at pH = 5.5. Precipitates were minor and mainly consisted of manganese oxides. The buffering mechanism in this section was coupled to the solid phase; if precipitates were removed, the pH increase was steeper, i.e. less base had to be added, and buffering was much less effective. Figure 2 depicts the curve of continuous titration compared to a titration curve with separation of precipitates at pH = 4 after the addition of 9.2 mmol L^{-1} NaOH. The steep increase of the titration curve after the separation of precipitates (at ≈ 12 mmol L^{-1} NaOH) indicates the decisive influence that surface effects have on buffering. Investigating the alteration of precipitate composition between pH = 5.0 and 8.5 gives further indications of the buffering mechanism (Figure 3). The acidic precipitate at pH = 5 contained considerable amounts of SO_4, but no Ca and Mg. In contrast, the alkaline precipitate at pH = 8.5 clearly contained Ca and Mg and distinctly less SO_4. Sulphate release as well as adsorption of Ca and Mg both release hydrogen ions and could cause the section IV buffering.

Modelling

Modelling was used to investigate if these processes could quantitatively explain the observed buffering. The following input parameters were required:

- Composition of the initial acidic solution
- Fe and Al hydroxysulphate stoichiometries
- Solubility products of the precipitating phases
- Surface complexation reactions with their thermodynamic data
- number of exchange sites on the hydrous ferric surface

The model parameterisation for the Plessa 111 mining lake is summarised in Table 1. Ion activities for the lake water composition were calculated with PHREEQC, according to the Debye-Hückel model.

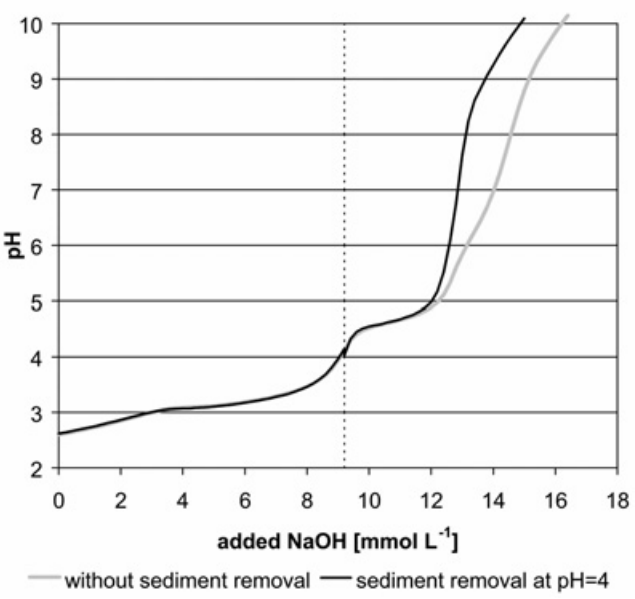

Figure 2. Comparison of titration curves of the continuous titration and of the titration with sediment removal after addition of 9.2 mmol L^{-1} NaOH.

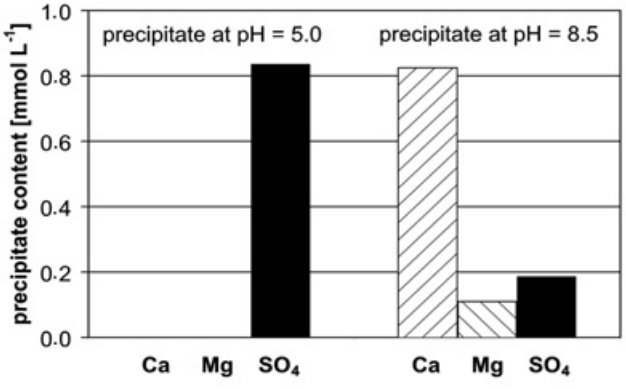

Figure 3. The amounts of calcium, magnesium, and sulphate in the precipitating sediment during the titration up to pH = 5 and up to pH = 8.5.

The solubility products of iron hydroxide or schwertmannite, respectively, and aluminium hydroxysulphate were fitted to the buffering plateaus of the titration curve. Iron and aluminium hydroxysulphate stoichiometries were calculated from measured Fe/S and Al/S molar ratios in the precipitates. The exchange capacity of precipitating iron hydroxides was adjusted in such a way that using the intrinsic thermodynamic dissociation constants for iron hydroxide as well as the complexation constants for SO_4 given in PHREEQC led to a good reproduction of measured surface-complexed SO_4 contents. In general, there was a good agreement between these values and literature values (Table 2). For iron hydroxide, a pK_{sp} of 4.0 was determined, which is in line with a pK_{sp} of 4.9 for amorphous ferrihydrite. For iron oxyhydroxysulphate, the derived pK_{sp} was 21.0, which is similar to the pK_{sp} for

schwertmannite, 18 ± 2.5. The determined pK_{sp} for aluminium hydroxide is 9.0, and thus in between the values for amorphous aluminium hydroxide (10.8) and gibbsite (8.1). Finally, for aluminium hydroxy-sulphate, a pK_{sp} of 5.0 was derived, which is close to the pK_{sp} of 5.7 for basaluminite. Equations and thermodynamic data for surface exchange were taken from Dzombak and Morel (1990), as implemented in the WATEQ4F.dat data base of PHREEQC, with minor modifications for Ca and Mg (Table 1C).

Sensitivity Analysis

The inaccuracy of model input parameters was accounted for in a sensitivity analysis. The most sensitive parameters for the shape of the titration curve are the concentrations of free hydrogen ions, which is characterised by the pH of the initial solution, the aqueous Fe^{3+} and Al^{3+} concentrations, and the sulphur content in the precipitates. The following uncertainties were assumed: starting pH, ± 0.05 units; Fe and Al concentrations, ± 5%; and S content, ± 20%.

Modelled Titration Curves

Modelled titration curves are shown in Figure 4. In each plot, the measured curve was plotted together with the simulated curve and the uncertainty interval associated with the analyses. The first titration curve (Figure 4A), derived with the hydroxide model, shows two plateaus. The Fe buffer sets in at pH ≈ 3 and the Al buffer at pH ≈ 4.5. Compared to the measured curve, however, the plateaus are distinctively too long.

In addition, there is no buffering in section IV of the titration curve. Consequently, the hydroxide model is too simple to quantitatively describe the neutralisation of the lake water. The hydroxide model does not account for SO_4 in the precipitating phases.

In Figure 4B, the precipitation of Fe and Al hydroxy-sulphates instead of hydroxides leads to a shortening of the Fe and Al buffer plateaus, better approximating the measured curve. The pH rise after the Al buffer, however, is still much too steep. The buffer plateau lengths are shorter because when SO_4 substitutes for the hydroxide ions, less hydrogen ions are released per mole of Fe or Al (Table 1B).

Figure 4C illustrates SO_4 binding by surface complexation, which is reversible, in contrast to the

Table 1. Model parameterisation including precipitation and surface exchange reactions

A. Initial Solution

Parameter	Value
pH	2.55
Sodium	0.31 mmol L^{-1}
Potassium	0.08 mmol L^{-1}
Magnesium	1.10 mmol L^{-1}
Calcium	4.64 mmol L^{-1}
Iron	2.68 mmol L^{-1}
Aluminium	1.05 mmol L^{-1}
Manganese	0.06 mmol L^{-1}
Sulphate	13.63 mmol L^{-1}
Chloride	0.25 mmol L^{-1}

B. Phase Models

Model	Precipitation reaction	pK_{sp}
hydroxide model	$Fe^{3+} + 3\ H_2O \rightarrow Fe(OH)_3 + 3\ H^+$	4
	$Al^{3+} + 3\ H_2O \rightarrow Al(OH)_3 + 3\ H^+$	9
hydroxysulphate model	$8\ Fe^{3+} + 1.44\ SO_4^{2-} + 13.12\ H_2O \rightarrow Fe_8O_8(OH)_{5.12}(SO_4)_{1.44} + 21.12\ H^+$	21
	$Al^{3+} + 0.37\ SO_4^{2-} + 2.26\ H_2O \rightarrow Al(OH)_{2.26}(SO_4)_{0.37} + 2.26\ H^+$	5
surface complexation model	$Fe^{3+} + 3\ H_2O \rightarrow Fe(OH)_3 + 3\ H^+$	4
	$Al^{3+} + 0.37\ SO_4^{2-} + 2.26\ H_2O \rightarrow Al(OH)_{2.26}(SO_4)_{0.37} + 2.26\ H^+$	5
all models	$Mn^{2+} + 2\ H_2O \rightarrow MnO_2 + 4\ H^+ + 2\ e^-$	-43.6

C. Surface Exchange Processes (Dzombak and Morel 1990)

	Reaction	pK
protonation / deprotonation	$Hfo\text{-}wOH + H^+ \rightarrow Hfo\text{-}wOH_2^+$	-7.29
	$Hfo\text{-}wOH \rightarrow Hfo\text{-}wO^- + H^+$	8.93
sulphate	$Hfo\text{-}wOH + SO_4^{2-} + H^+ \rightarrow Hfo\text{-}wSO_4^- + H_2O$	-7.78
	$Hfo\text{-}wOH + SO_4^{2-} \rightarrow Hfo\text{-}wOHSO_4^{2-}$	-0.79
base cations [1]	$Hfo\text{-}wOH + Ca^{2+} \rightarrow Hfo\text{-}wOCa^+ + H^+$	5.15
	$Hfo\text{-}wOH + Mg^{2+} \rightarrow Hfo\text{-}wOMg^+ + H^+$	4.60
exchange sites	0.6 mol sites / mol $Fe(OH)_3$	

Hfo-w denotes the weak binding sites of hydrous ferric oxides; [1] Fitted to measurements.

Table 2. Solubility products of iron and aluminium hydroxides and hydroxysulphates in the literature

	Mineral	Precipitation reaction	pK_{sp}	
Fe	amorphous ferrihydrite	$Fe^{3+} + 3\ H_2O \rightarrow Fe(OH)_3 + 3\ H^+$	4.9	[1]
	schwertmannite	$8\ Fe^{3+} + SO_4^{2-} + 14\ H_2O \rightarrow Fe_8O_8(OH)_6SO_4 + 22\ H^+$	18 ± 2.5	[2]
	amorphous Al-hydroxide	$Al^{3+} + 3\ H_2O \rightarrow Al(OH)_3 + 3\ H^+$	10.8	[1]
Al	gibbsite	$Al^{3+} + 3\ H_2O \rightarrow Al(OH)_3 + 3\ H^+$	8.1	[1]
	basaluminite	$Al^{3+} + 0.25\ SO_4^{2-} + 2.5\ H_2O \rightarrow Al(OH)_{2.5}(SO_4)_{0.25} + 2.5\ H^+$	5.7	[1]

[1] Parkhurst and Appelo 1999; [2] Bigham et al. 1996

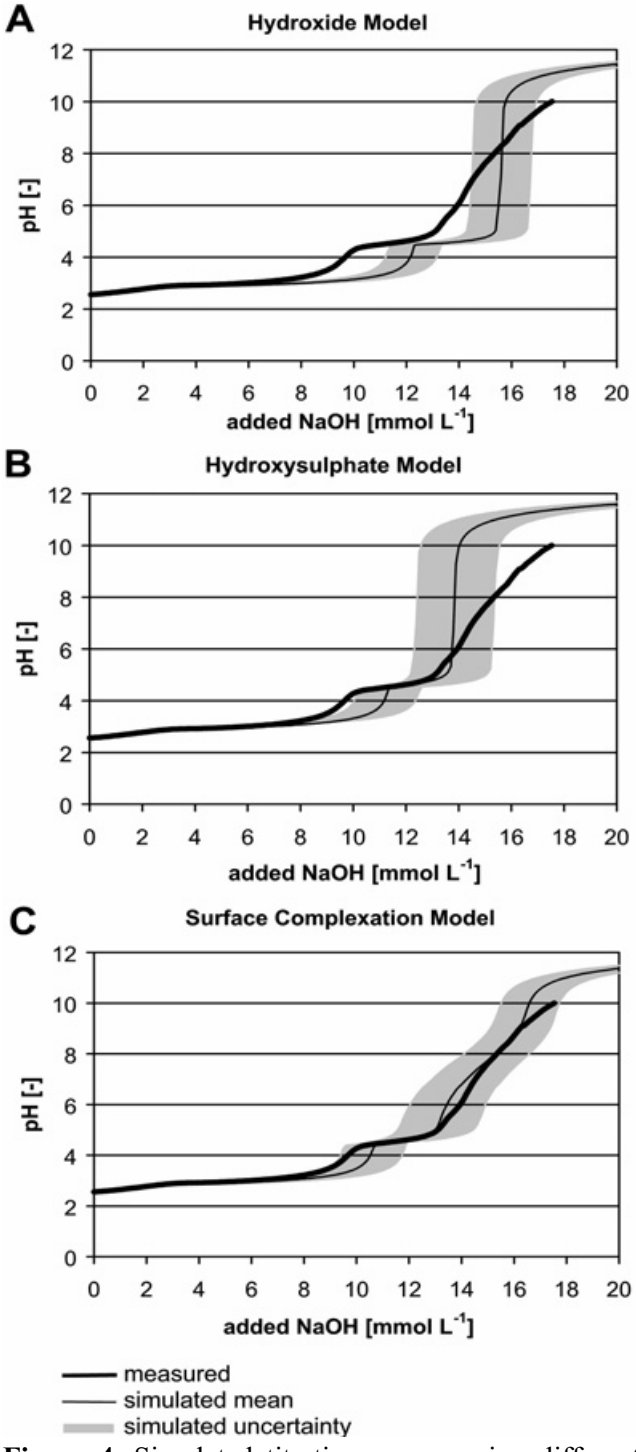

Figure 4. Simulated titration curves using different model assumptions with respect to solid phase reactions (see text)

hydroxysulphate model. Like the second model, the surface complexation model has shorter Fe and Al buffer plateaus than the hydroxide model, but it also shows a pronounced buffering in the last section of the titration curve, and thus best approximates the measured titration curve. The shortening of Fe and Al buffer plateaus in the model is due to SO_4 and hydrogen ion adsorption in the acidic environment (Figure 5). Both processes remove hydrogen ions from the solution and therefore cause an earlier rise in pH (Table 1C). Between pH = 5 and 8, SO_4 and hydrogen ions are released again from the solid phase and Ca and Mg are bound, leading to an additional buffering effect in the neutral pH range.

Titration curves were recorded under continuous stirring, i.e. in an open system. However, there was no equilibrium between the solution and the

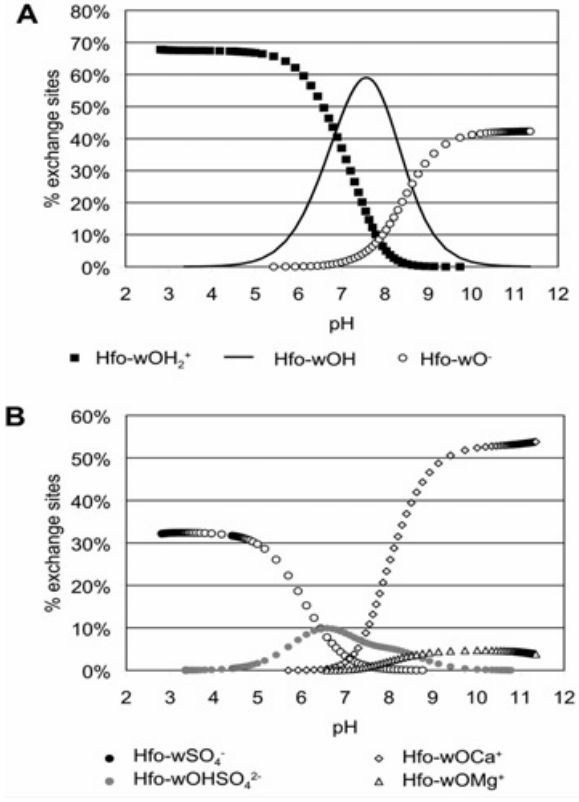

Figure 5. Distribution of species on the surface of iron hydroxide at varied pH values using the surface complexation model and standard parameterisation given in Table 1. (Hfo-w denotes the weak binding sites on the hydrous ferric oxide surface.)

atmosphere with respect to CO_2. According to the model calculations, equilibrium with the atmosphere with respect to CO_2 would lead to the formation of carbonic acid buffering at pH > 7 and even to the precipitation of calcium carbonate at pH > 8 (Figure 6). The carbonic acid /carbonate buffer, however, was not observed in the titration experiments. This indicates that CO_2 delivery is limited in the laboratory experiments at the time scale of a few hours to a few days. Therefore, CO_2 was neglected in the model calculations. This simplification, though, only applies to the laboratory experiments and not to the field.

Experiments and model calculations demonstrate the important role of SO_4 in the precipitates. SO_4 leads to a shortening of the Fe and Al buffer plateaus. Only by taking SO_4 in the precipitates into account is it possible to explain the lengths of the measured buffer plateaus. Concerning the type of SO_4 binding, some questions remain unresolved. Phase analyses point to the fact that the precipitating phases are iron hydroxysulphate (schwertmannite) and aluminium hydroxysulphate in the acidic environment. On the other hand, a comparison of the acidic precipitate at pH = 5.0 with the alkaline precipitate at pH = 8.5 (Figure 3) shows that SO_4 is released from the solid phase during titration and that Ca and Mg are bound. This observation favours surface binding.

Combining both suggests that iron and aluminium hydroxysulphates precipitate in the acidic environment and are then transformed to hydroxides or hydrooxides during the titration, whereby the previously bound SO_4 is released. Such a mineral transformation is known to take place during the ageing of schwertmannite (Bigham et al. 1996). Considering the overall chemistry with respect to buffering, both mineral transformation (Equation 1) and SO_4 desorption (Equation 2) release hydrogen ions. Together with the adsorption of Ca and Mg, these act as additional buffering mechanisms in the neutral pH range.

The transformation from schwertmannite to goethite is a kinetically controlled process. In a strongly acidic environment, the mineral transformation is a long-lasting process, taking years (Bigham et al. 1996). We do not know how much time it takes in the weakly acidic and neutral environment. In contrast to mineral transformation, surface complexation can be approximated as an equilibrium process. As the titration experiments did not show any substantial

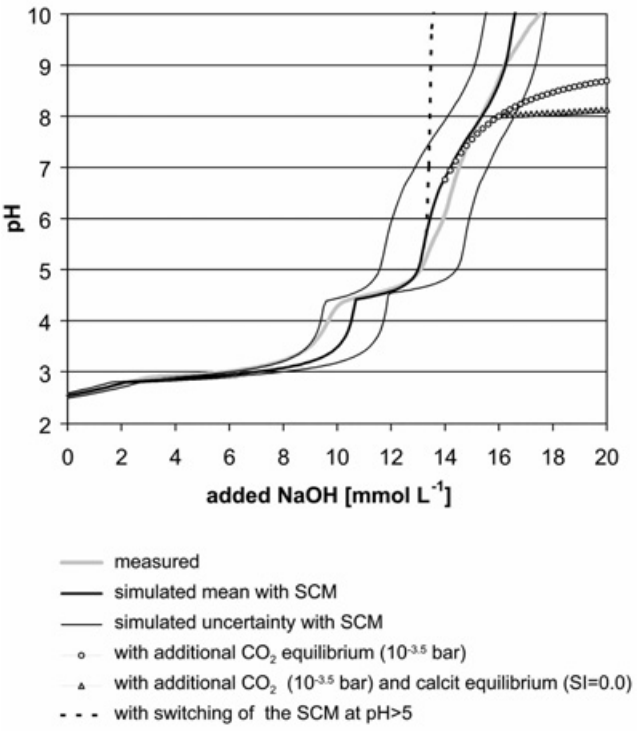

Figure 6. Comparison of different chemical models for the buffering at pH>5. (SCM denotes the surface complexation model for iron hydroxide.)

time dependency, we favour the concept of surface complexation for a model-based description of buffering mechanisms.

The conservative balance of the ion-specific acidity accounting for complex compounds (e.g. hydroxy complexes) and activity coefficients (Table 3) results in approximately the same alkalinity demand for neutralisation up to pH = 8.2 as does the model-based balance of the acidity considering solid-bound SO_4 and surface exchange processes (Table 4). However, the course of buffering is different (Figure 7), which is important in the context of controlling the processes in the field. Surface complexation of free hydrogen ions and SO_4 ions on iron hydroxides leads to a maximum shortening of approximately 1.5 meq L^{-1} of the Fe buffer plateau. The process is obviously reversible if the sediment remains in the system. At increasing pH up to approximately 8, this shortening of the buffer plateau is almost completely compensated by desorption of SO_4. The precipitation of aluminium hydroxysulphate terminates at pH ≈ 5.5. SO_4 binding leads to a shortening of the Al buffer plateau of approximately 0.8 meq L^{-1}. In addition to SO_4 desorption, at pH > 7, deprotonation of iron hydroxides and the surface complexation of Ca and Mg on iron hydroxides,

$$Fe_8O_8(OH)_{5.12}(SO_4)_{1.44} + 2.88\ H_2O \rightarrow 8\ FeOOH + 2.88\ H^+ + 1.44\ SO_4^{2-} \quad (1)$$

$$Hfo\text{-}wSO_4^- + Hfo\text{-}wOH_2^+ + H_2O \rightarrow 2Hfo\text{-}wOH + 2H^+ + SO_4^{2-} \quad (2)$$

(charge balanced acidic environment) (neutral environment)

Table 3. Conservative values of buffering

Parameter	Produced Acidity	pH Range of Buffering
Hydrogen ion [1]	3.2 meq L^{-1}	2.55...4.3
Hydrogen sulphate	1.3 meq L^{-1}	2.55...4.3
Iron(III) [2]	7.7 meq L^{-1}	2.55...3.5
Aluminium [2]	3.2 meq L^{-1}	4.5...5.5
Carbonic acid	< 0.1 meq L^{-1}	4.3...8.2
Sum	15.4 meq L^{-1}	2.55...8.2

[1]Considering the ion activity coefficient; [2] considering the hydroxy complexes at pH = 2.55

increase buffering. Up to pH ≈ 8.2, there is an additional alkalinity demand of approximately 0.7 meq L^{-1}.

We assume that aluminium hydroxides exhibit the same properties as iron hydroxides with respect to surface complexation. However, thermodynamic data are not available for surface complexation on aluminium hydroxides. This mainly affects titration curves in the neutral and alkaline range (pH > 6) and may lead to an underestimation of the surface complexation buffer in the model. The buffer intensity is defined as the degree to which pH changes when alkalinity is added (Stumm and Morgan 1996):

$$\beta = -d(pH)/dAlk_{add})$$

Figure 8 depicts the measured and modelled buffer intensity, which agree well up to pH ≈ 9.

Conclusions

The experimental results and model calculations on the acidic lake water lead to several conclusions. First, the titration curve can be divided into four sections: (1) the neutralisation of free hydrogen ions and hydrogen sulphate deprotonation; (2) homogeneous and heterogeneous Fe^{3+} buffering with SO_4 binding; (3) homogeneous and heterogeneous Al buffering with SO_4 binding and; (4) buffering by surface exchange processes. Buffering by carbonic acid was not a factor.

Second, SO_4 that co-precipitates with the Fe and Al mineral phases distinctively shortens the buffer plateaus in the acidic range.

Third, at pH > 5, buffering processes occur that are based on surface effects of the precipitating phases. These lead to a damped increase of the titration curve.

Finally, a phase model consisting of ferrihydrite, aluminium hydroxysulphate, and manganese oxide with surface complexation of SO_4, Ca, and Mg on the ferrihydrite surface proved to be suitable for a quantitative description of the measured titration curve, indicating that surface complexation on fresh

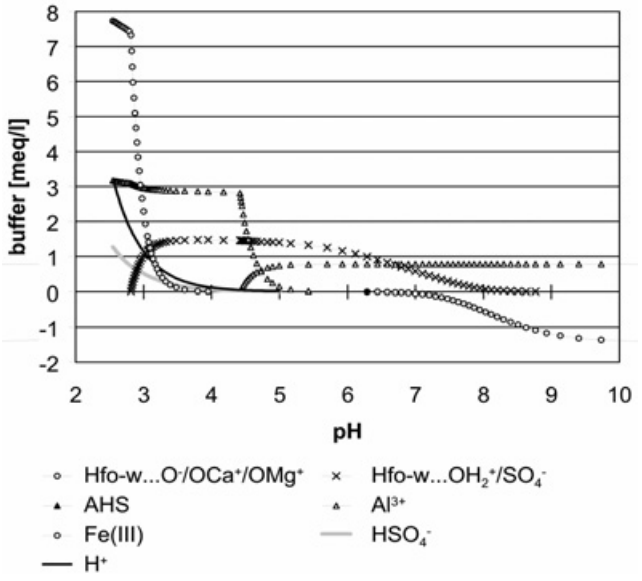

Figure 7. pH-dependent concentrations of acidity and alkalinity bearing components, and surface reactions in the lake water (calculated with PHREEQC; model 3)

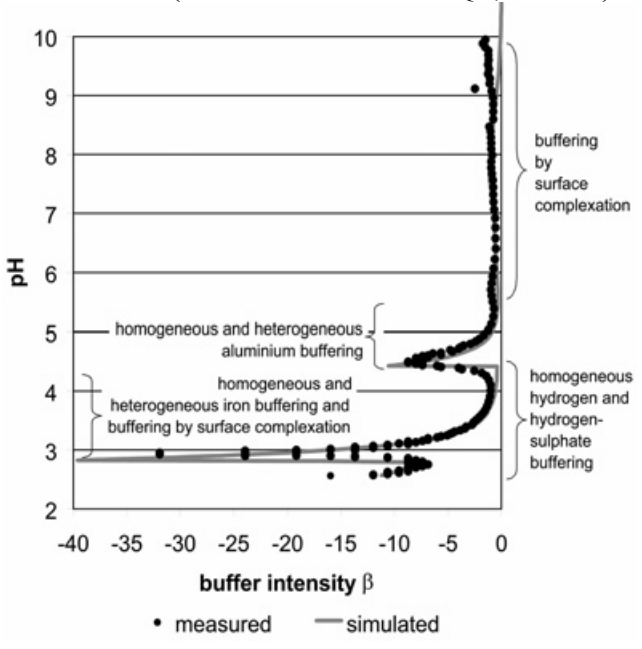

Figure 8. Buffer intensity of the buffering processes for the measured and the simulated titration curve.

precipitates plays an important role during the neutralisation of acidic mining lake water.

Acknowledgements

We thank the laboratory staff of the Leibniz-Institute of Freshwater Ecology and Inland Fisheries for their help with the chemical analyses. The study was funded by the German Ministry of Education and Research, BMBF, and the mining restoration corporation, LMBV (BMBF-FKZ 0339746, LMBV-Best.-Nr. 45016514), and by the German Federal Environment Foundation (DBU).

Table 4. Buffering values, considering surface complexation and aluminium hydroxysulphate precipitation

Parameter	Produced Acidity	Consumed Acidity	pH Range of Buffering
Hydrogen ion [1]	3.2 meq L^{-1}		2.55...4.3
Hydrogen sulphate	1.3 meq L^{-1}		2.55...4.3
Iron(III) [2]	7.7 meq L^{-1}		2.55...3.5
Hfo-w...OH_2^+/SO_4^-		-1.5 meq L^{-1}	2.8...3.8
Aluminium [2]	3.2 meq L^{-1}		4.5...5.5
AHS		-0.8 meq L^{-1}	4.5...5.5
Hfo-w...OH_2^+/SO_4^-	1.5 meq L^{-1}		3.8...8.2
Carbonic acid	<0.1 meq L^{-1}		4.3...8.2
Hfo-w…$O^-/OCa^+/OMg^+$	0.7 meq L^{-1}		6.5...8.2
Sum	15.3 meq L^{-1}		2.55...8.2

[1] Considering the ion activity coefficient; [2] considering the hydroxy complexes at pH = 2.55

References

Bigham JM, Schwertmann U, Carlson L, Murad E (1990) A poorly crystallized oxyhydroxy sulfate of iron formed by bacterial oxidation of Fe(II) in acid mine waters. Geochimica et Cosmochimica Acta 54: 2743-2758

Bigham JM, Schwertmann U, Traina SJ, Winland RL, Wolf M (1996) Schwertmannite and the chemical modeling of iron in acid sulfate waters. Geochimica et Cosmochimica Acta 60(12): 2111-2121

Dzombak DA, Morel FMM (1990) Surface complexation modelling – Hydrous ferric oxide. John Wiley & Sons, NY, 393 p

Fyson A, Kalin M (2000) Acidity Titration Curves – a Versatile Tool for the Characterisation of Acidic Mine Waste Water. In: UFZ-Bericht 6, Umweltforschungszentrum Leipzig-Halle, Leipzig, pp 21-24

Geller W, Klapper H, Schultze M (1998) Natural and Anthropogenic Sulfuric Acidification of Lakes. In: Geller W, Klapper H, Salomons W (eds) Acidic Mining Lakes. Springer Verlag, Berlin, pp 3-14

Grünewald U (1999) Aktuelle Probleme des Wasserdargebotes bezüglich Menge und Beschaffenheit in der Niederlausitz. Wasserkalender 33: 28-47

Klapper H, Geller W, Schultze M (1996) Abatement of acidification in mining lakes in Germany. Lakes & Reservoirs: Research and Management 2: 7-16

Klapper H, Friese K, Scharf B, Schimmele M, Schultze M (1998) Ways of controlling acid by ecotechnology. In: Geller W, Klapper H, Salomons W (eds) Acidic Mining Lakes, Springer Verlag, Berlin, pp 401-418

Nixdorf B, Hemm M, Schlundt A, Kapfer M, Krumbeck H (2001) Braunkohlentagebauseen in Deutschland. Umweltbundesamt Texte 35/01, Berlin,

Nixdorf B, Lessmann D, Steinberg CEW (2003) The importance of chemical buffering for pelagic and benthic colonization in acidic waters. Water, Air and Soil Pollution 3: 27-46

Parkhurst DL, Appelo CAJ (1999) Users's Guide to PHREEQC (Version 2). USGS WRI Report 99-4259, Denver, 312 p

Schnoor JL, Galloway JN, Moldan B (1997) East central Europe: an environment in transition. Environ Science and Technol 31: 412A-416A

Skousen J, Rose A, Geidel G, Foreman J, Evans R, Hellier W et al. (1998) Handbook of Technologies for Avoidance and Remediation of Acid Mine Drainage. West Virginia University, Morgantown, WV, 131 p

Stumm W, Morgan JJ (1996), Aquatic chemistry. Chemical equilibria and rates in natural waters. John Wiley & Sons, NY, 1022 p

Totsche O, Steinberg CEW (2003) Suche nach Neutralisationsstrategien für extrem saure Tagebauseen - eine Literaturstudie. Vom Wasser 100: 111-140

Totsche O, Fyson A, Steinberg CEW (2002) Chemical and Microbial neutralization of extremely acidic mining lakes – buffering of extreme acidic mining lakes. Proc, Water Resources and Environment Research, Dresden, Germany, 170-173

Totsche O, Pöthig R, Uhlmann W, Büttcher H, Steinberg CEW (submitted) Buffering Mechanisms in Acidic Mining Lakes – a Model-Based Analysis. Aquatic Geochem

Uhlmann W, Nitsche C, Neumann V, Guderitz I, Leßmann D, Nixdorf B, Hemm M (2001) Tagebauseen: Wasserbeschaffenheit und Wassergütebewirtschaftung - Konzeptionelle Vorstellungen und erste Erfahrungen. Studien und Tagungsberichte 35, Landesumweltamt Brandenburg, Potsdam, 77 p

Ulrich B (1981) Die Rolle der Wälder für die Wassergüte unter dem Einfluß des sauren Regens. Agrarspektrum 2: 212-231

Received November 6, 2003; accepted February 6, 2004